

RESEARCH ARTICLE

Editorial Process: Submission:09/28/2023 Acceptance:02/20/2024

Investigation of *in-vitro* Anti-Cancer and Apoptotic Potential of Garlic-Derived Nanovesicles against Prostate and Cervical Cancer Cell Lines

Vinayak Sharma, Eshu Singhal Sinha, Jagtar Singh*

Abstract

Objective: Investigate the anti-cancerous potential of garlic-derived nanovesicles (GDNVs), exploring their cytotoxic effects on HeLa and PC-3 cell lines, and elucidate the underlying mechanisms, including apoptosis induction and inhibition of epithelial-mesenchymal transition (EMT). **Methods:** GDNVs were isolated using differential centrifugation and ultracentrifugation. Characterization was performed through dynamic light scattering (DLS), field-emission scanning electron microscopy (FESEM), and Fourier-transform infrared spectroscopy (FTIR). Cytotoxicity assessments on HeLa and PC-3 cell lines using MTT assay. Apoptosis induction was evaluated through nuclear morphology changes and quantification of apoptotic cells using DAPI and PI/annexin V analysis. Western blot of apoptosis-related proteins (bcl-2, bax, caspase-3) was analysed. Anti-metastatic potential was assessed using wound healing assay and EMT transition inhibition. **Results:** Garlic-derived nanovesicles (GDNVs), characterized by a size of 134.2 nm, demonstrated a substantial and dose- as well as time-dependent anti-proliferative impact on HeLa and PC-3 cell lines. The induction of apoptosis was unequivocally established through discernible modifications in nuclear morphology. The apoptotic cell count in HeLa and PC-3 cells increased by $42.4 \pm 4.2\%$ and $38.2 \pm 3.2\%$, respectively. Comprehensive Western blot demonstrated alterations in the expression of key apoptotic regulators, namely bcl-2, bax, and caspase-3, providing robust evidence for the initiation of apoptosis. Furthermore, GDNVs exerted a significant inhibitory effect ($p < 0.001$) on the migratory potential of both HeLa and PC-3 cells. Moreover, there was a discernible association between GDNVs and the suppression of Epithelial-Mesenchymal Transition (EMT), emphasizing their role in impeding the metastatic potential of these cancer cell lines. **Conclusion:** This study establishes, for the first time, the anti-cancerous potential of GDNVs. The observed dose- and time-dependent anti-proliferative effects, selective cytotoxicity, apoptosis induction, and anti-migratory potential highlight GDNVs as a promising candidate for cancer treatment.

Keywords: Prostate cancer- cervical cancer- nanovesicles- apoptosis- metastasis

Asian Pac J Cancer Prev, **25** (2), 575-585

Introduction

The global health landscape faces significant challenges with cervical and prostate cancers, profoundly influencing cancer-related mortality. Cervical cancer, primarily affecting women, holds the fourth position among the most prevalent cancers in females worldwide [1]. Prostate cancer, primarily impacting men, stands as the second most frequently diagnosed cancer globally. As reported by the World Health Organization in 2020, cervical cancer in women accounted for around 604,000 new cases and 342,000 deaths [2]. In the United States during 2021, approximately 248,530 new cases of prostate cancer in men were diagnosed, resulting in about 34,130 deaths [3, 4]. These cancers present challenges, including late-stage diagnosis, restricted access to screening and early detection methods, socioeconomic disparities, and low awareness, all contributing to increased mortality rates

[5, 6]. Current treatment options for cervical and prostate cancers have limitations, such as adverse side effects and the emergence of drug resistance [7]. Consequently, there is an urgent need to investigate innovative therapeutic approaches that can effectively tackle these malignancies.

Extensive research has focused on exploring the diverse array of bioactive compounds found in plants, showcasing their therapeutic potential against a range of diseases, including cancer [8, 9]. Epidemiological investigations have highlighted the capabilities of nanosized extracellular vesicles derived from edible plants, illustrating their role in influencing cell function and transporting various biomolecules between cells [10]. Moreover, these vesicles are naturally released by a variety of fruits and vegetables, contributing to health-promoting effects [11].

Several studies indicate that certain nanovesicles surpass conventional active components in efficacy

Department of Biotechnology, Panjab University, Chandigarh, India. *For Correspondence: jagtar72@gmail.com

due to their distinctive lipid composition and vesicular surface potential, enhancing their targeting to disease sites and accumulation. For instance, nanovesicles derived from turmeric exhibit superior wound healing potential in CaCo2 cells compared to curcumin alone [12]. These nanovesicles demonstrate various medicinal properties, including antioxidant [13], anti-inflammatory [14] (B. Liu et al., 2020;), anti-aging [15], and anti-cancer activities [16]. Notably, exosome-like nanovesicles from tea leaves, as demonstrated by Q. Chen et al. [17], were found to suppress the proliferation of breast cancer cells by inducing cell cycle arrest and apoptosis. Additionally, studies by Raimondo et al. [18] and Yang et al. [19] revealed that nanovesicles isolated from lemon possess anti-cancer properties against colorectal and gastric cancers, respectively. These findings underscore the potential of plant-derived nanovesicles as emerging agents in the field of anticancer drugs, leveraging the diverse chemical compositions and biological activities inherent in natural products [20].

Allium sativum, commonly known as garlic, is widely consumed edible plant known for its beneficial effects on human health. It is used in traditional medicines for centuries. It is known to contain bioactive molecules mainly organosulfur compounds such as allicin, ajoene, diallyl sulphides (DAS), diallyl disulphides (DADS) and diallyl trisulphides (DATS). These bioactive molecules impart anti-inflammatory, anti-diabetic, anti-fungal, anti-viral, anti-protozoal, anti-microbial, anti-cancer, and cardioprotective properties to garlic [21, 10]. Consumption of a large amount of allium vegetables has proven to inhibit gastric cancer, esophageal cancer, prostate cancer, and cancer of the pharynx, larynx, renal cells, breast, ovary, and endometrium [22-25]. Although the anti-cancerous potential of garlic is extensively studied, the effect of garlic-derived nanovesicles (GDNVs) on prostate and cervical cancer has not been demonstrated and remains unexplored.

In this context, the present study has been employed for the isolation of GDNVs via differential centrifugation method and deciphered the inherent anticancer properties by employing in vitro cell culture models of cervical and prostate cancer and evaluated the effects of nanovesicle treatment on cell viability, apoptosis induction, and caspase activation and furthermore demonstrated the effect of GDNVs on the cancer cell migration and epithelial to mesenchymal transition (EMT) which is the hallmark of metastasis.

Materials and Methods

Nanovesicle preparation

Garlic was procured from the local market. Nanovesicles were isolated from the cloves of garlic using differential centrifugation followed by the ultracentrifugation method. Garlic cloves were subjected to homogenization using a high-speed blender for 1 minute. The collected garlic juice was centrifuged sequentially at 3,000g for 20 minutes and then at 10,000g for 1 hour at 4°C to remove debris. Then the supernatant was subjected to filtration using a 0.45µm membrane filter. The filtered suspension was then

pelleted by ultra-centrifugation at 120,000g for 1 hour at 4°C using an SW28 Ti Beckmann rotor. The supernatant was discarded followed by washing with cold phosphate-buffered saline (PBS). The pellet was subsequently resuspended in PBS and subjected to filtration using a 0.22 µm membrane filter and followed by ultra-centrifugation at 120,000g for 2 hours. The isolated nanovesicles were resuspended in cold PBS and stored at -80°C till further use. Protein concentrations were measured by BCA assay using a BCA kit (G-biosciences) [26].

Characterization of nanovesicles

The size distribution of the nanovesicles was assessed utilizing dynamic light scattering (DLS) through the employment of a Malvern Zetasizer (version 7.04). The nanovesicles that had been successfully isolated were subjected to visualization procedures employing field emission scanning electron microscopy (FESEM). To facilitate this, the nanovesicles were resuspended in a solution of phosphate-buffered saline (PBS). Subsequently, nanovesicles were affixed onto coverslips and then fixed onto stubs for examination. Following this, air drying was carried out, after which a thin coating of gold was applied over the samples for a duration of 30 seconds. This gold coating procedure was performed utilizing an MC 1000 ion sputter coater procured from Hitachi, Japan. The subsequent assessment of nanovesicle morphology was conducted utilizing an SU 8010 scanning electron microscope, also manufactured by Hitachi, Japan, in accordance with the methodology described by [27]. For the comprehensive determination of the chemical constituents and functional groups present within the nanovesicles, Fourier transform infrared (FTIR) spectroscopy was employed. This analytical technique was executed using a model RZX FTIR spectrometer manufactured by Perkin Elmer [28]. Through this methodology, the specific organic compounds and functional groups were elucidated, affording a deeper understanding of the nanovesicle composition and structure.

Cell culture

HeLa, PC-3, and HEK-293 cells were procured from the cell repository of the National Centre for Cell Science (Pune, India). All cell lines used in the study were grown in RPMI-1640 media supplemented with 10% FBS (fetal bovine serum) and antibiotics (100 U/ml penicillin, 100 µg/ml streptomycin) from HiMedia. The cells were maintained at 80% confluency at 37°C in a humidified atmosphere with 5% CO₂.

MTT assay

MTT assay was performed as previously described [29]. Briefly, 1×10⁴ cells/well was seeded in triplicates in 96 well cell culture plates. Next day the cells were treated with GDNVs (50 - 300µg/ml) for 24, 48, and 72 hours. Untreated cells were used as control. Subsequently, 20µl of MTT (5mg/ml) was added to each well of a plate. After 4 hours the culture media was removed and the purple color formazan crystals were dissolved in 100µl of DMSO per well. The absorbance was determined at 540nm with the

help of a microplate reader (Synergy H1, Biotek).

Colony formation assay

A colony formation assay was performed as described [30] with minor modifications. Briefly, 2000 cells were seeded in each well of 6 well cell culture plate. After 24 hours the cells were treated with GDNVs for 48 hours or left untreated. After 7 days the cells were washed with PBS and fixing of cells was done using 6% glutaraldehyde for 1 hour at 4°C. Subsequently, crystal violet (0.5%) was used for 8 min to stain the colonies. A digital camera was employed for obtaining the images of stained colonies. For quantitative analysis, the bound crystal violet colonies were solubilized using 30% glacial acetic acid, and a BioTek microplate reader was used to measure the absorbance at 570nm. The percentage of the colony-forming efficiency of nanovesicles treated and untreated cells was plotted.

DAPI staining

DAPI staining was performed as described [31]. Briefly, the cells were seeded in 6-well plates containing cover slips and the cells were treated with GDNVs at a concentration of 200µg/ml. After 48 hours, cells were fixed with 4% paraformaldehyde for 10-15 minutes, washed thrice with PBS, and subsequently permeabilized for 10 minutes with 0.1% Triton X-100. Furthermore, cells were subjected to PBS wash and then the staining of cells was done using 300nM DAPI (4, 6-diamidino-2-phenylindole) for 5 minutes. For the evaluation of cells fluorescent microscope (Nikon) was used at 20 X magnification.

PI-AnnexinV assay

Apoptosis analysis was done using a PI Annexin V kit (BD, biosciences). For this, both HeLa and PC-3 cells were subjected to GDNVs treatment at a concentration of 200µg/ml for 48 hours. The cells were washed thrice with PBS and resuspended in 100 µl 1X Annexin V binding buffer (0.1M HEPES/NaOH, pH-7.4, 1.4M NaCl, 25 mM CaCl₂). 0.7µl of Annexin V and 1µl of PI were added to the cells. The cells were vortex gently and incubated for 15 minutes in the dark at room temperature. 400µl of binding buffer was added to each sample followed by the acquisition of the sample using flow cytometry FACS Calibur (BD Biosciences San Jose, CA). FlowJo software (Tree Star, Ashland OR) was employed for the analysis of results [7]. Cells positive for both PI-AnnexinV were considered as apoptotic cells.

Wound Healing Assay

For wound healing analysis both HeLa and PC-3 (5×10⁵ cells/well) were seeded in 6 well plates. After 90% of the confluency was achieved then wound was created in the cell's monolayer manually. RPMI 1640 culture medium were supplemented with 100 µg/ml GDNVs were added. At 0 and 48 hour after GDNVs treatment, the morphology of the cells were observed using inverted microscope. The area of cells migration was measured using Image-J software. The wound areas were calculated as:

(value of area at 0 h- value of area at 48 h)/ (value of area at 0 h)%

Western blot

The cells were lysed as described by [32] with minor modifications. Briefly, culture cells were collected and washed with ice cold phosphate-buffered saline (PBS) and subsequently resuspended in an ice-cold lysis buffer (Cell Signaling Technology, USA). The lysis buffer was supplemented with a cocktail of protease inhibitors and phenylmethanesulfonyl fluoride (PMSF) to ensure the preservation of protein integrity during the lysis process. This suspension was allowed to incubate on ice for a period of 20-30 minutes, a critical step to ensure efficient disruption of cellular membranes. The ensuing lysates were subjected to centrifugation at 14,000 rpm for 10 minutes at 4°C. The quantification of protein content in the lysates was executed employing the Bicinchoninic Acid (BCA) assay. Subsequently, 80 µg of protein was loaded onto polyacrylamide gels for SDS-PAGE, a technique that resolves proteins based on their molecular weights. Western blot was performed as described [33]. Briefly, proteins from the SDS gel were transferred to Amersham protran nitrocellulose membrane (GE healthcare) using a semi dry system (Bio-Rad, USA). The unbound sites were blocked with 5% dried milk in PBS-T. This also prevents nonspecific binding of primary Ab. The membrane was washed thrice with PBS-T. Blots were probed with primary Abs (1:3000 for Bcl-2, bax, β-actin, and 1: 2000 dilutions were used for caspase-3, E-cadherin and vimentin) (Santa Cruz Biotechnology, USA) by incubating overnight at 4°C. After a similar washing step, the membranes were incubated with 1:2000 dilution of HRP-conjugated goat α mouse Ab for 1 h at RT. Binding of HRP-conjugated secondary Abs was determined using enhanced chemiluminescent substrate from G Biosciences; and the signals were captured on X-ray films. Densitometric analysis was performed using ImageJ software (National Institutes of Health).

Statistical Analysis

The data were expressed as mean + SD from at least three independent experiments. The statistical analyses were carried out using Graph-pad Prism 5 and the student's t-test, one-way ANOVA, and Dunnet's t-test. P values less than 0.05 are considered significant.

Results

Isolation and characterization of GDNVs

GDNVs were isolated using differential centrifugation followed by ultracentrifugation method. To determine the size of isolated nanovesicles dynamic light scattering (DLS) was employed as shown in Figure 1a. The result indicates that the average size of the GDNVs was 134.2 nm. Furthermore, to confirm the size and morphology of the isolated nanovesicles FESEM was used. FESEM analysis indicates that the nanovesicles were 100-200 nm in size and were spheroid in shape (Figure 1b).

Subsequently, FTIR spectroscopy was employed for the demonstration of the organic compounds present in

the GDNVs based on the FTIR transmittance spectrum. FTIR analysis reveals that the major transmittance peaks were at 3285.1, 2926.6, 1648.3, 1454.4, 1064.1, 988.3, and 861.1 cm^{-1} (Figure 1c). These peaks are indicative of the existence of N-H, O-H, C=C, C-H, C-N, and OCH₃ functional groups based on the standard IR spectrum (Table 1).

GDNVs induce cytotoxicity and inhibit colony formation in prostate and cervical cancer cells

MTT assay was used for the demonstration of the effect of GDNVs on the viability and growth of cancer cells. Both PC-3 and HeLa cells were treated with increasing concentrations (50 $\mu\text{g/ml}$ -300 $\mu\text{g/ml}$) of GDNVs for 24, 48, and 72 hours. The results indicated that GDNVs showed a significant inhibition of both prostate and cervical cancer cells in a dose and time-dependent manner (Figure 2a and b). The cytotoxic effect of GDNVs was clearly evitable at 50 $\mu\text{g/ml}$ concentration after 24 hours treatment on both cell lines. However, 50% growth reduction was observed at 200 $\mu\text{g/ml}$ concentration of GDNVs after 48 hours. Furthermore, the study also evaluated the specificity of nanovesicles derived from garlic against cancer cells by testing their effect on non-cancerous cells HEK-293. The results indicate that the inhibitory effect of GDNVs is specific to cancer cells as non-cancerous cells HEK-293 was found to be less affected (10.68%) at highest concentration of GDNVs (300 $\mu\text{g/ml}$) (Figure 2c). Based on these findings, the subsequent analysis was conducted using a concentration of 200 $\mu\text{g/ml}$ for a 48-hours incubation period.

The effect of GDNVs on in vitro tumor growth was evaluated using a colony formation assay. Cells were treated with 200 $\mu\text{g/ml}$ of nanovesicles. The results shown in Figure 3 suggest that GDNVs significantly suppressed the colony-forming potential of HeLa by $70.1 \pm 3.4\%$ (Figure 3a) and PC-3 by $63.8 \pm 2.8\%$ (Figure 3b) as compared to untreated cells. This suggests that the GDNVs have an inhibitory effect on the ability of cancer cells to form colonies, thereby suppressing their tumor growth in vitro.

GDNVs induce apoptosis in prostate and cervical cancer cells

To elucidate the cytotoxic effect of GDNVs in cancer cells were due to apoptosis induction, we employed two different methods, PI annexin V and DAPI staining (Figure 4 and 5). The PI/AnnexinV assay was performed using flow cytometry. This assay allows the identification

Table 1. Peak Values of GDNVs FTIR Spectra in the Region of 650-4000 cm^{-1}

Wavenumbers (cm^{-1})	Peak values	Chemical bond
2500-3300	3285	N-H and C-H
2500-3300	2926.6	N-H and C-H
1638-1648	1648.3	C=C, C-N, C=O
1330-1420	1454.4	O-H
1000-1250	1064.1	C-N and C-O
985-995	988.3	C=C and OCH ₃
880 \pm 20	861.1	C-H

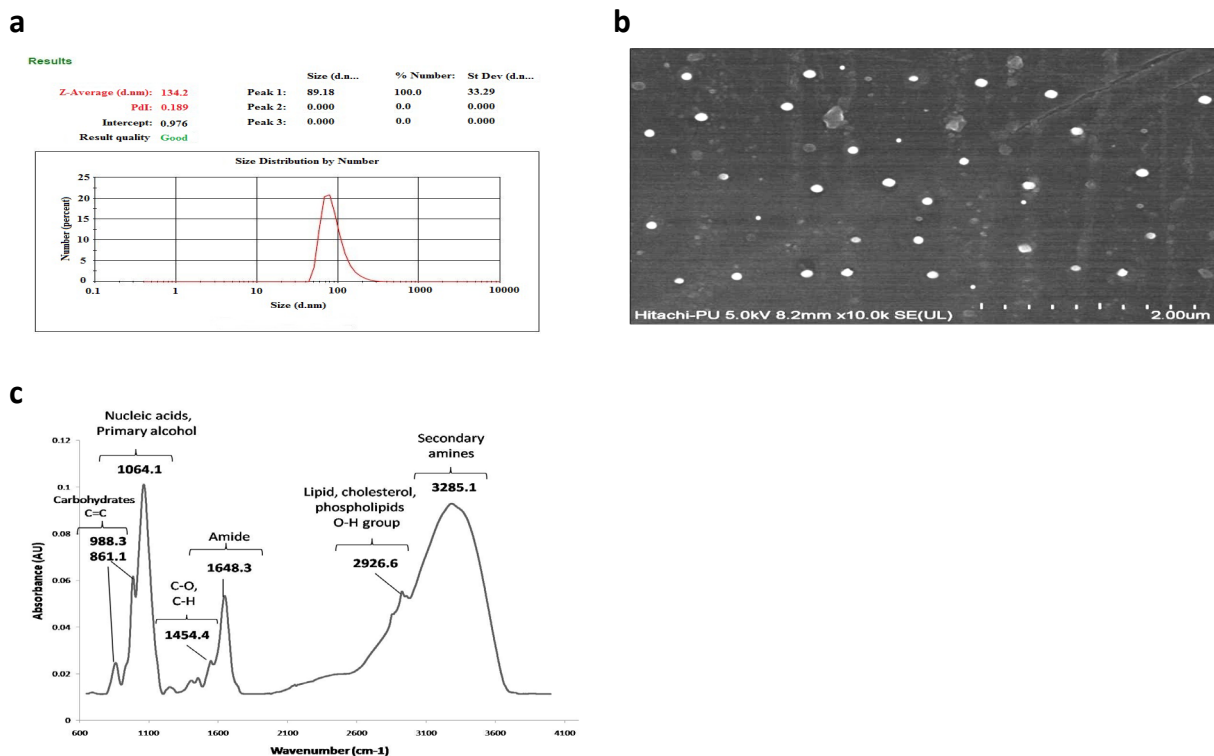


Figure 1. Characterization of GDNVs. (a) Dynamic light scattering (DLS) was employed for the evaluation of the size distribution of GDNVs. (b) Morphology of GDNVs depicted using FESEM. Scale bar = 2 μm . (c) FTIR spectra of GDNVs.

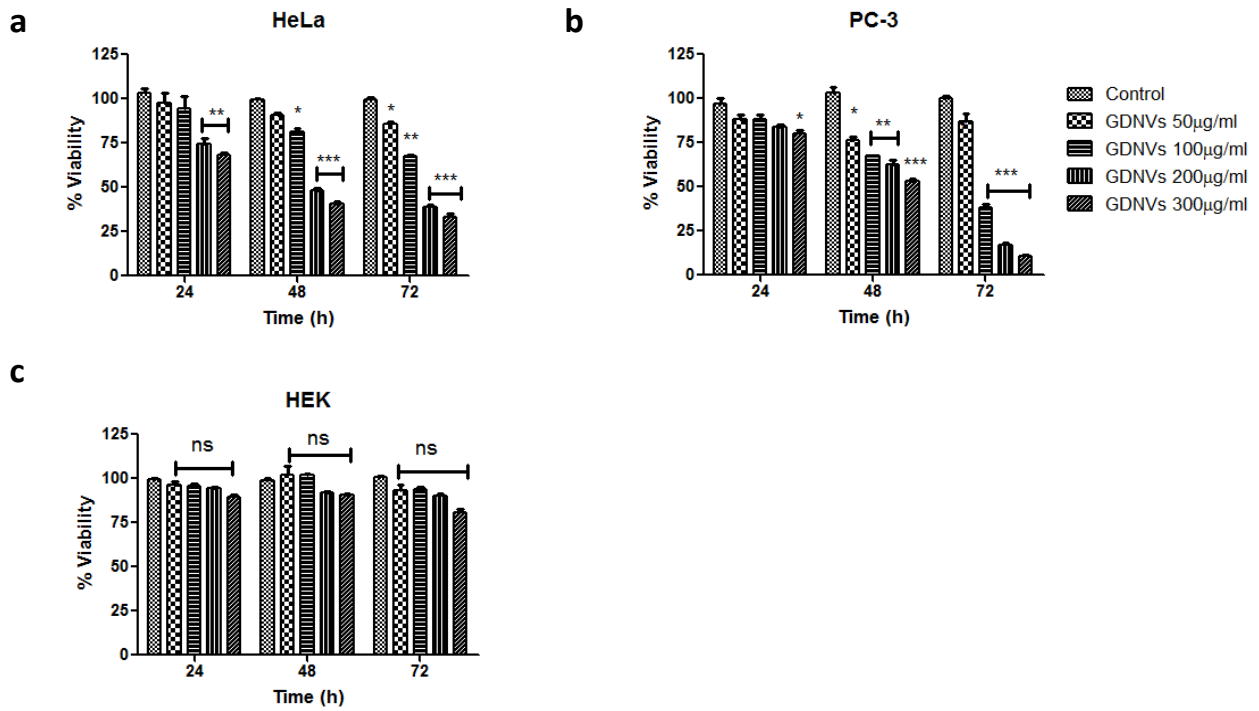


Figure 2. GDNVs Suppress the Growth of Cancer Cells. Cell viability of (a) HeLa (b) PC-3 and (c) HEK-293 was measured by MTT assay after 24, 48, and 72 hours of treatment with 50µg/ml, 100µg/ml, 200µg/ml, and 300µg/ml of GDNVs. The data represented as % viability and the experiment was performed in triplicate and presented as the mean + standard deviation. In comparison to the control statistically significant values were represented by an asterisk (* $p < 0.05$; ** $p < 0.01$; *** $p < 0.001$).

and quantification of apoptotic cells based on their binding to specific markers. The results of the PI/annexin V assay depict that the percentage of apoptotic cells has significantly augmented in both cell lines. In HeLa cells,

$42.4 \pm 4.2\%$ of cells were apoptotic, compared to only $8.7 \pm 2.1\%$ in the control cells (Figure 4a). Similarly, in PC-3 cells, $38.2 \pm 3.2\%$ of cells were apoptotic, compared to $10.7 \pm 2.4\%$ in the control cells (Figure 4b). To further

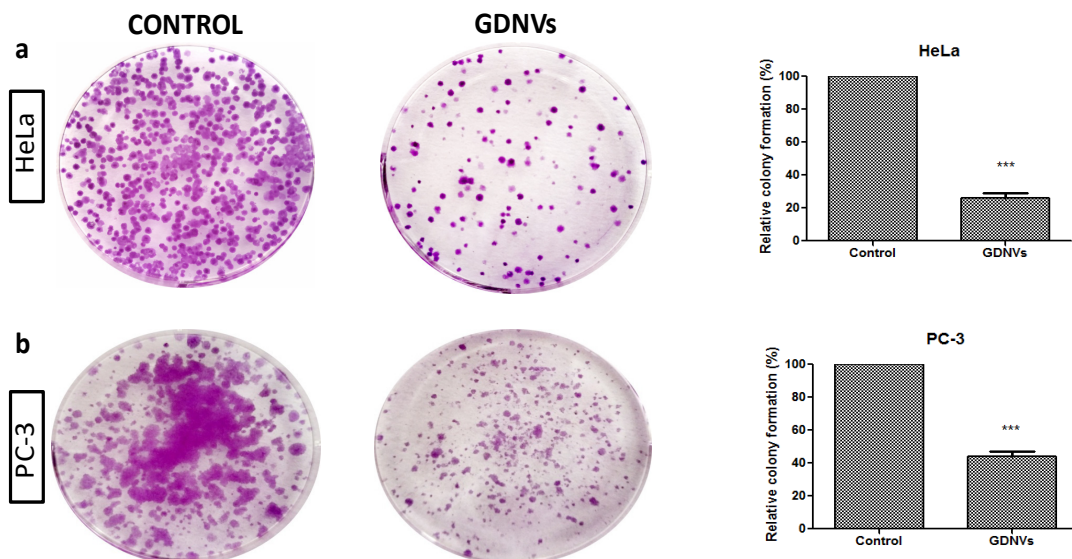


Figure 3. GDNVs Inhibit Colony Formation in Cancer Cell Lines. Effect of GDNVs on the colony-forming potential of (a) HeLa and (b) PC-3 cells were detected. Cells were treated with 200µg/ml GDNVs or left untreated. Representative images and a bar graph showing quantification of the colony-forming potential of prostate and cervical cancer cells. The experiment was performed in triplicate and presented as the mean \pm S.D; *** $P < 0.001$ compared with controls. In comparison to the control, statistically significant values were represented by an asterisk (* $p < 0.05$; ** $p < 0.01$; *** $p < 0.001$).

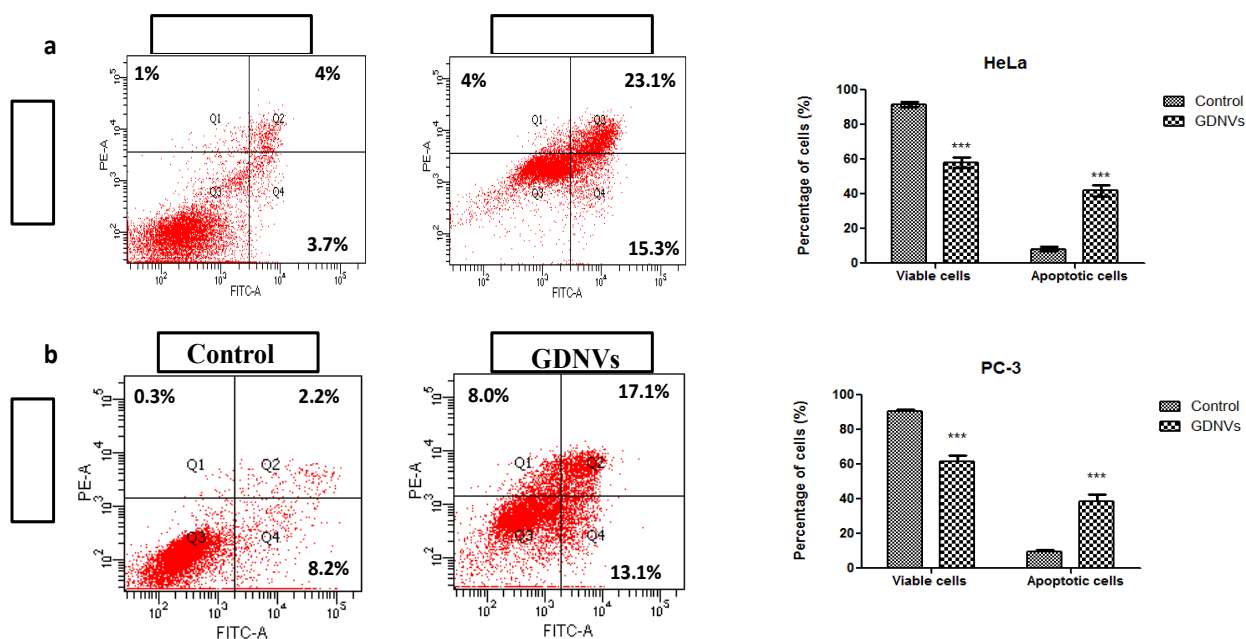


Figure 4. GDNVs Induce Apoptosis in Prostate and Cervical Cancer Cells. PI/annexin V staining and further analysis by flow cytometry dot plots in (a) HeLa and (b) PC-3 cells respectively showing induction of apoptosis after 48 hours. Data expressed as the mean \pm S.D. Asterisk represents the statistically significant values in comparison to control (* $p < 0.05$; ** $p < 0.01$; *** $p < 0.001$).

confirm the induction of apoptosis we employed DAPI staining where cancer cells used in the study were treated with 200 μ g/ml of GDNVs and followed by 48 hours incubation. After incubation, the cells were stained with DAPI, a fluorescent dye that binds to DNA. The results, as shown in Figure 5, indicated a significant induction of apoptosis in the nanovesicle-treated cells. Distorted nuclear peripheries were clearly visible in these cells, suggesting cellular changes associated with apoptosis.

In contrast, the control cells exhibited uniformity in size, shape, and intact nuclei. These findings collectively suggest that the GDNVs inhibit prostate and cervical cancer cell proliferation by inducing apoptosis.

GDNVs trigger apoptosis via activation of bax and caspase-3

In order to further confirm the underlying mechanism responsible for the anti-cancerous effect of GDNVs,

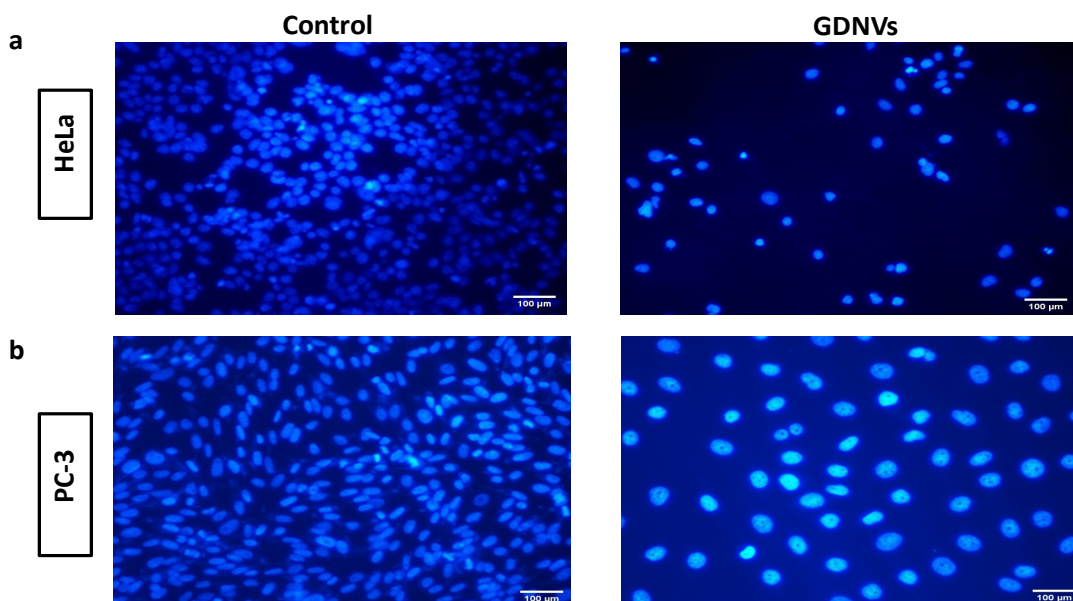


Figure 5. DAPI Staining Shows the Induction of Apoptosis. (a) HeLa, (b) PC-3 cells are treated with 200 μ g/ml of GDNVs for 48 hours or left untreated. Apoptosis was confirmed by DAPI staining which showed apparent changes in nuclear morphology (chromatin condensation and morphological distortions) of HeLa and PC-3, respectively. The experiment was performed in triplicate. Scale bar = 100 μ m.

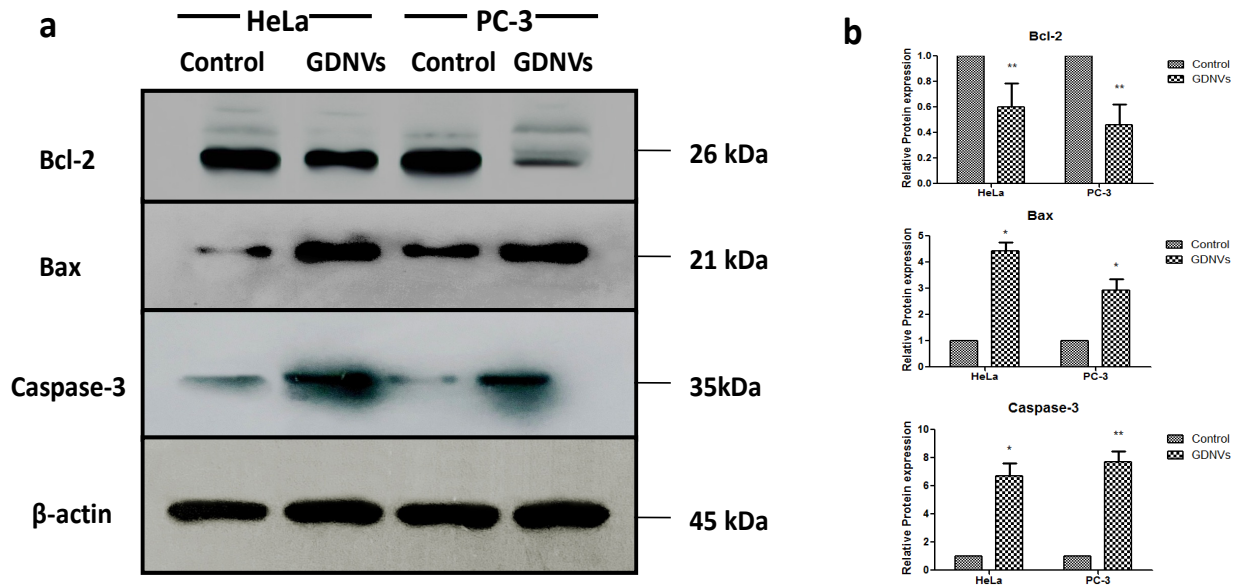


Figure 6. Alteration in the Expression of Proteins Associated with Apoptosis. (a) Representative blots and (b) densitometric analysis of proteins in HeLa and PC-3 cells after GDNVs treatment at a concentration 200 μ g/ml. β -actin was used for normalization in western blotting. Untreated cells were taken as control with the basal level as indicated as 1. The data is indicated as mean \pm S.D with n=3. Asterisk represents the statistically significant values in comparison to control (*p < 0.05; **p < 0.01; ***p < 0.001).

we performed a western blot analysis. We evaluated the impact of GDNVs on the expression levels of key apoptosis-regulating proteins, namely Bcl-2, Bax, and caspase-3 induced by GDNVs. We treated the cells with 200 μ g/ml of GDNVs and analyzed the protein expression. Treatment with GDNVs led to an increase in the expression of the pro-apoptotic protein Bax,

which promotes apoptosis (Figure 6). At the same time, it resulted in a decrease in the expression of the anti-apoptotic protein Bcl-2, which typically inhibits apoptosis (Figure 6). Furthermore, we evaluated the effect of GDNVs on caspase-3 protein expression level using western blot analysis. The results demonstrated a significant augmentation in the expression level of

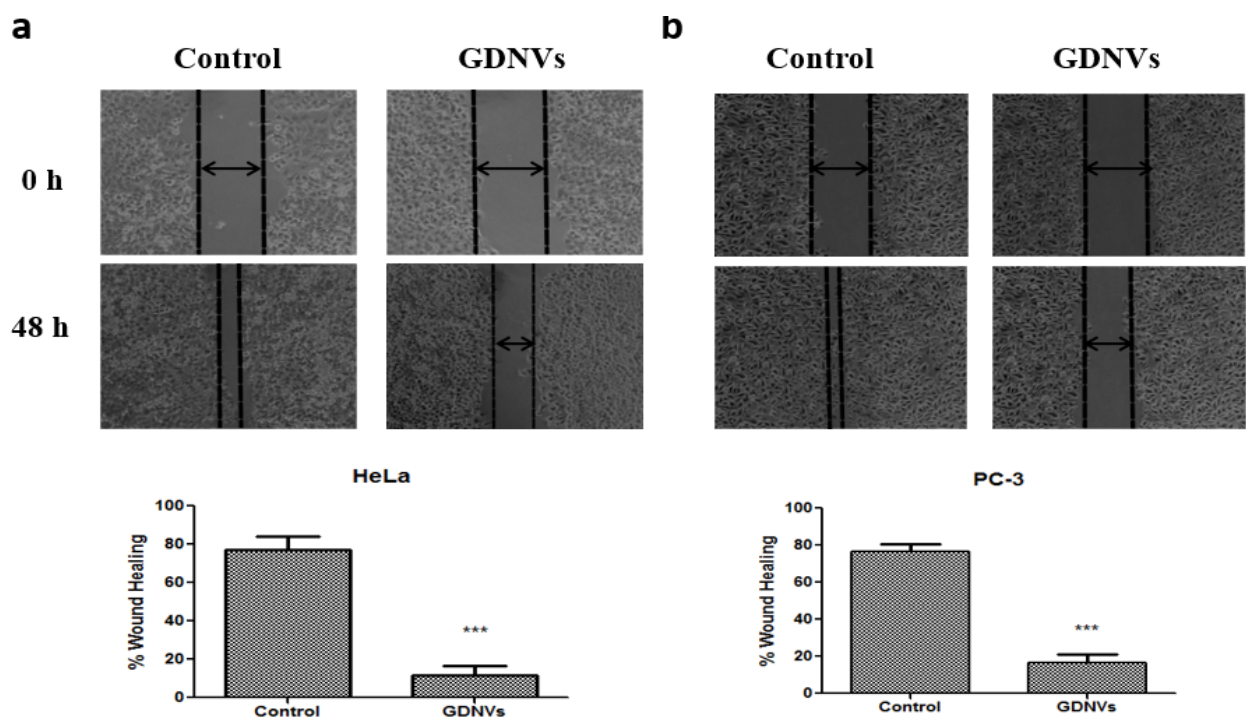


Figure 7. Inhibition of Migration of HeLa (a), and PC-3 (b), with treatment of 200 μ g/ml of GDNVs for 48hours. Histogram depicting the percentage of wound healing in untreated and treated cells expressed as mean \pm S.D. (n = 3). The data was analyzed by one way ANOVA test. **P<0.01, ***P<0.001.

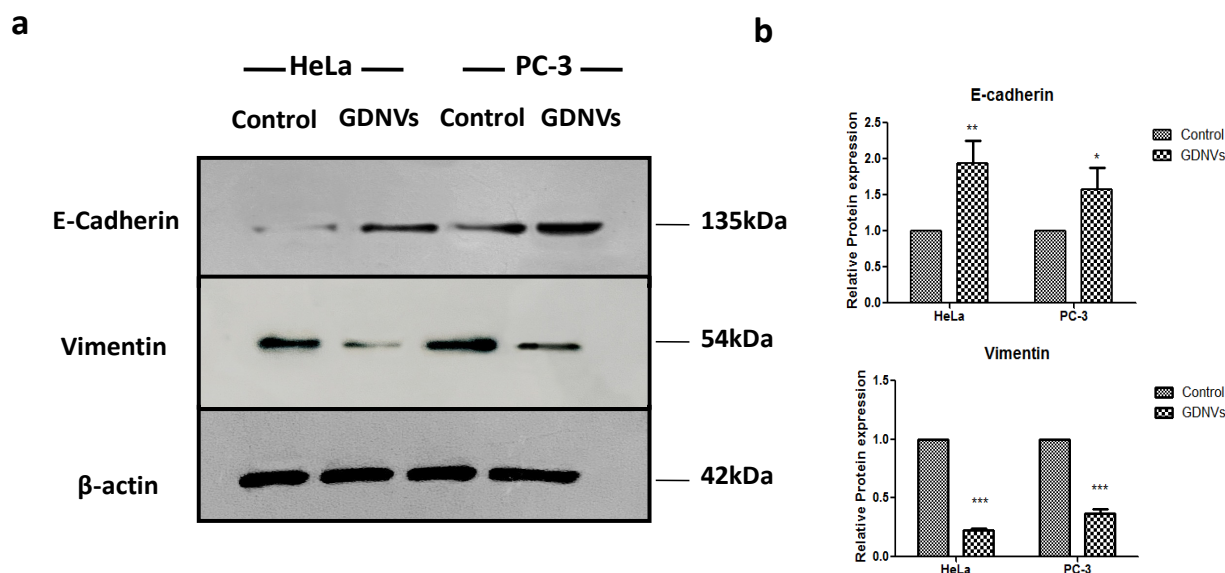


Figure 8. Alteration in the Expression of Proteins associated with EMT Transition. (a) Representative blots and (b) densitometric analysis of proteins in HeLa and PC-3 cells after GDNVs treatment at a concentration 200µg/ml. β-actin was used for normalization in western blotting. Untreated cells were taken as control with the basal level as indicated as 1. The data is indicated as mean± S.D with n=3. Asterisk represents the statistically significant values in comparison to control (*p < 0.05; **p < 0.01; ***p < 0.001).

caspase-3 in the nanovesicles-treated cells compared to the untreated cells (Figure 6). This upregulation of caspase-3 indicates the initiation of apoptosis in the GDNVs-treated cells.

In a nutshell, our results indicate that GDNVs impart an inhibitory effect on both HeLa and PC-3 cancer cells by activation of apoptosis, mainly by regulating the protein expression level of bcl-2, bax, and caspase-3.

GDNVs suppress the cancer cell's migration via suppression of EMT

Metastasis is a process by which cancer cells spread from the primary site of the tumor site to other parts of the body through the bloodstream since migration is the primary step in metastasis, therefore, using wound healing assay, we evaluated the effect of GDNVs on the migration of different cancer cells. The results showed that treating the cells with nanovesicles led to a significant reduction in the closure of the wound compared to untreated cells, indicating nanovesicles inhibit the migration of cells. The percentage of wound healing varied depending on the type of cancer cells (Figure 7). For HeLa only 11.6 ± 5.1% (Figure 7a), while for PC-3 i.e. 16.5 ± 4.5% (Figure 7b) wound healing with respect to untreated cells at 200µg/ml for 48 hours. However, these findings pointed toward the anti-metastatic role of GDNVs. Since epithelial to mesenchymal transition (EMT) is a process in which epithelial cells transformed into mesenchymal cells which is a crucial process for cancer metastasis therefore, we next investigated the effect of the GDNVs on the expression of EMT related proteins in both cancer cell lines by western blot analysis. The results showed in Figure 8 that at 200µg/ml of GDNVs treatment for 48 hours significantly reduced the expression of mesenchymal marker vimentin in both HeLa and PC-3 cancer cells, whereas, there is significant

augmentation of the expression of epithelial marker E-cadherin as compared to untreated cells. These findings indicated the role of GDNVs in inhibition of metastasis via suppression of EMT process.

Discussion

Despite significant progress in cancer research, cancer remains a leading cause of death worldwide, highlighting the need for continued efforts to discover and develop anticancer medicines. Although multiple molecular compounds have been examined for their chemotherapeutic and chemo-protective effects in various cancer types such as prostate, colon, breast, and stomach carcinogenesis in vitro and in vivo, but the hunt for newer and more effective treatments continues [34]. Numerous data in the literature showed that various edible plants such as ginger, garlic, turmeric, and mushrooms have been used in traditional medicine and have been found to possess anti-proliferative effect against various types of cancer [35, 36, 19]. However, the molecular mechanisms underlying these anti-proliferative activities are not fully understood. Garlic is consumed worldwide in different food recipes and also known to possess several pharmacological activities including antibacterial, antioxidant, anti-diabetic and immunoprotective effects [21]. However, no studies were reported for the anticancerous effects of GDNVs.

Numerous evidences supports that the secretion of exosome like vesicles by plants shares similar properties with mammalian- derived nanovesicles. For example, a study by An et al. [37] demonstrated that plants secrete vesicles that are similar in size and morphology to mammalian nanovesicles, and that these vesicles contain proteins and RNA. While the function of these

plant-derived exosome-like vesicles is not yet fully understood. Interestingly, a growing body of evidence indicates that these plant-derived EVs exhibit a remarkable capacity for internalization by specific mammalian cells, such as intestinal stem cells, macrophages, and cancer cells [38, 11, 5]. They play a pivotal role in facilitating cross-kingdom communication between plants and animals, mediating the transfer of endogenous bioactive molecules to recipient cells and triggering intricate cellular and molecular responses [39]. For instance, Mu et al. [40] have reported that grape-derived nanoparticles were able to enter mouse intestinal macrophages, thus inducing the expression of anti-oxidant genes and suppressing the production of pro-inflammatory cytokines. Consequently, plant-derived EVs have emerged as promising candidates for therapeutic applications

Therefore, in this study we isolated the nanovesicles from garlic to determine whether these nanovesicles are capable of imparting anti-cancerous effects. Subsequently in this present study, we isolated and characterized nanovesicles derived from garlic for the first time and chose two cancer cell lines HeLa, and PC-3, for evaluating the effects of nanovesicle treatment on cell proliferation and cell survival.

In the current study we isolated nanovesicles firstly by using differential centrifugation followed by ultracentrifugation method. The DLS data reveals that the isolated nanovesicles were 134.2 nm in diameter and FESEM analysis revealed that the nanovesicles were spheroid in shape. These results are corroborated with studies of [17] and Şahin et al. [27] where they isolated nanovesicles from tea flower, wheat and ginger which are spheroid in shape with size ranges from 50-200 nm.

FTIR is a powerful technique used to study the vibrational modes of molecules in the mid-infrared region (400-4000 cm^{-1}). This technique provides a unique fingerprint of a sample's composition, allowing for the identification of different chemical compounds. The FTIR spectrum of nanovesicles derived from buffalo milk indicated several mid-infrared spectral regions, such as the amide band (1300-1700 cm^{-1}) are of particular interest for the analysis of proteins. These bands are sensitive to the secondary structure of proteins, providing information on the presence of alpha-helices, beta-sheets and random coils. Similarly, C-H regions (2700-3500 cm^{-1}) are of interest, as they are sensitive for the presence of lipids and carbohydrates. The FTIR spectral bands within 900-1200 cm^{-1} is mainly due to phosphodiester groups of nucleic acids and phospholipids and the C-O absorption of some carbohydrates [28]. Similarly, in case of garlic vesicular suspension the FTIR measurements have revealed the prominent absorbance band that can be attributed to various components of GDNVs including proteins, lipids, carbohydrates and polysaccharides.

Furthermore, we investigated the anti-cancerous potential of GDNVs by measuring their effect on cancer cells using MTT assay. MTT assay suggested that nanovesicles exhibit anti-cancerous activity in a dose-dependent manner against both cancer cell lines, as it suggests that the nanovesicles may have broad spectrum anti-cancer activity. However nanovesicles showed lesser

effect on normal HEK293 cell line, as it suggests that the nanovesicles may have selective cytotoxicity against cancer cells. These findings are consistent with previous studies by Q. Chen et al. [17] and Wongkaewkhaw et al. [41].

Tumor clonality refers to a process by which a single cell undergoes genetic mutations that results in uncontrolled cell division and the formation of tumor. Understanding tumor clonality is important for developing effective cancer treatment. Subsequently, we investigated the effect of GDNVs on the colony forming potential of cancer cells using colony forming assay. The results suggested that GDNVs significantly inhibits the cell proliferation of cancer cells used in the study. These findings are corroborated with Raimondo et al. [18] and Yang et al. [26] where lemon derived nanovesicles and extracellular vesicles inhibits the colony formation potential of tumor cell lines and gastric cancer cells.

In the process of apoptosis, nuclear DNA undergoes fragmentation and condensation, resulting in alterations to chromatin structure [42]. To substantiate the anti-proliferative effects of GDNVs through apoptosis, DAPI staining revealed distorted nuclear peripheries in nanovesicle-treated cells compared to controls. Moreover, the PI/annexin V assay confirmed a significant increase in both early and late apoptotic cells in HeLa and PC-3 cells treated with nanovesicles compared to untreated cells. These findings are in line with the observations made by Chen et al. [17], where they demonstrated the induction of apoptosis by GDNVs in lung cancer cells.

Additionally, Bcl-2 family proteins, known for their dual roles in apoptosis regulation, play a pivotal role in cell death [43]. Treatment with GDNVs significantly decreased bcl-2 levels and increased bax expression, leading to an elevated bax/bcl-2 ratio indicative of pro-apoptotic signaling. This is consistent with studies highlighting the crucial role of the bax/bcl-2 ratio in cancer cell apoptosis [44, 41]. The heightened bax/bcl-2 ratio suggests that GDNVs may activate the intrinsic apoptosis pathway, potentially causing mitochondrial disruption, cytochrome C release, and initiator caspase-9 activation [45]. Subsequently, effector caspase-3, a key member of the caspase family, is activated, leading to apoptotic changes [1, 46]. GDNVs treatment also confirmed increased expression of caspase-3 in both HeLa and PC-3 cells.

Metastasis is a process in which cancer cells migrates to the other sites of the body to form new tumors. Since migration of the cancer cells to the different sites is the primary step in the initiation of the metastatic process [47]. Using wound healing assay we evaluated that GDNVs inhibit the cell migration potential in both HeLa and PC-3 cancer cells. Since epithelial to mesenchymal transition (EMT) is a process in which epithelial cells transformed into mesenchymal cells which is a crucial process for cancer metastasis [48] therefore, we next investigated the effect of the GDNVs on the expression of EMT related proteins in both cancer cell lines by western blot analysis. The results herein showed in Fig. 8 that at 200 $\mu\text{g/ml}$ of GDNVs treatment for 48 hours significantly reduced the expression of mesenchymal markers Vimentin in both HeLa and PC-3 cells, whereas, there is significant

augmentation of the expression of epithelial marker E-cadherin cancer cells as compared to untreated cells. These findings indicated the role of GDNVs in inhibition of metastasis via suppression of EMT process. Therefore, this validates the anti-metastatic role of GDNVs against cancer cells.

In conclusion, this study demonstrated for the first time that GDNVs possess anti-cancerous properties against cervical cancer and prostate cancer. We also demonstrated the anti-migratory potential of nanovesicles derived from garlic by wound healing assay and inhibition of EMT transition associated protein which is a hallmark of metastasis. These findings suggests that GDNVs could be a potential new alternative for the treatment of cancer.

Author Contribution Statement

Vinayak Sharma: Investigation, writing and editing original draft, review and editing original draft; Eshu Singhal Sinha: Supervision, review and editing original draft; Jagtar Singh: Supervision, review and editing original draft.

Acknowledgements

Funding statement

This work was supported by financial assistance to Vinayak Sharma from University Grant Commission, India.

Conflict of interest

Authors declared no competing interest.

Data availability

Authors declared that data is available within the manuscript.

Novelty Statement

Authors declare that work has not been the part of any thesis or published elsewhere.

References

1. Singh M, Jha RP, Shri N, Bhattacharyya K, Patel P, Dhammetiya D. Secular trends in incidence and mortality of cervical cancer in india and its states, 1990-2019: Data from the global burden of disease 2019 study. *BMC Cancer*. 2022;22(1):149. <https://doi.org/10.1186/s12885-022-09232-w>.
2. Singh P, Lim B. Targeting apoptosis in cancer. *Curr Oncol Rep*. 2022;24(3):273-84. <https://doi.org/10.1007/s11912-022-01199-y>.
3. Berenguer CV, Pereira F, Câmara JS, Pereira JAM. Underlying features of prostate cancer-statistics, risk factors, and emerging methods for its diagnosis. *Curr Oncol*. 2023;30(2):2300-21. <https://doi.org/10.3390/currenconcol30020178>
4. Al-Fayez S, El-Metwally A. Cigarette smoking and prostate cancer: A systematic review and meta-analysis of prospective cohort studies. *Tob Induc Dis*. 2023;21:19. <https://doi.org/10.18332/tid/157231>.
5. Wang B, Zhuang X, Deng ZB, Jiang H, Mu J, Wang Q, et al. Targeted drug delivery to intestinal macrophages by

- bioactive nanovesicles released from grapefruit. *Mol Ther*. 2014;22(3):522-34. <https://doi.org/10.1038/mt.2013.190>.
6. Hamdi Y, Abdeljaoued-Tej I, Zatchi AA, Abdelhak S, Boubaker S, Brown JS, et al. Cancer in africa: The untold story. *Front Oncol*. 2021;11:650117. <https://doi.org/10.3389/fonc.2021.650117>.
7. Majumder M, Debnath S, Gajbhiye RL, Saikia R, Gogoi B, Samanta SK, et al. Ricinus communis l. Fruit extract inhibits migration/invasion, induces apoptosis in breast cancer cells and arrests tumor progression in vivo. *Sci Rep*. 2019;9(1):14493. <https://doi.org/10.1038/s41598-019-50769-x>.
8. Dutta S, Mahalanobish S, Saha S, Ghosh S, Sil PC. Natural products: An upcoming therapeutic approach to cancer. *Food Chem Toxicol*. 2019;128:240-55. <https://doi.org/10.1016/j.fct.2019.04.012>.
9. Kaur R, Kapoor K, Kaur H. Plants as a source of anticancer agents. *J Nat Prod Plant Resour*. 2010;1:119-24.
10. Zhang Y, Liu X, Ruan J, Zhuang X, Zhang X, Li Z. Phytochemicals of garlic: Promising candidates for cancer therapy. *Biomed Pharmacother*. 2020;123:109730. <https://doi.org/10.1016/j.biopha.2019.109730>.
11. Ly NP, Han HS, Kim M, Park JH, Choi KY. Plant-derived nanovesicles: Current understanding and applications for cancer therapy. *Bioact Mater*. 2023;22:365-83. <https://doi.org/10.1016/j.bioactmat.2022.10.005>.
12. Liu C, Yan X, Zhang Y, Yang M, Ma Y, Zhang Y, et al. Oral administration of turmeric-derived exosome-like nanovesicles with anti-inflammatory and pro-resolving bioactions for murine colitis therapy. *J Nanobiotechnology*. 2022;20(1):206. <https://doi.org/10.1186/s12951-022-01421-w>.
13. De Robertis M, Sarra A, D'Oria V, Mura F, Bordini F, Postorino P, et al. Blueberry-derived exosome-like nanoparticles counter the response to tnf- α -induced change on gene expression in ea.Hy926 cells. *Biomolecules*. 2020;10(5). <https://doi.org/10.3390/biom10050742>.
14. Yin L, Yan L, Yu Q, Wang J, Liu C, Wang L, et al. Characterization of the microrna profile of ginger exosome-like nanoparticles and their anti-inflammatory effects in intestinal caco-2 cells. *J Agric Food Chem*. 2022;70(15):4725-34. <https://doi.org/10.1021/acs.jafc.1c07306>
15. Cho EG, Choi SY, Kim H, Choi EJ, Lee EJ, Park PJ, et al. Panax ginseng-derived extracellular vesicles facilitate anti-senescence effects in human skin cells: An eco-friendly and sustainable way to use ginseng substances. *Cells*. 2021;10(3). <https://doi.org/10.3390/cells10030486>.
16. Kim SQ, Kim KH. Emergence of edible plant-derived nanovesicles as functional food components and nanocarriers for therapeutics delivery: Potentials in human health and disease. *Cells*. 2022;11(14). <https://doi.org/10.3390/cells11142232>
17. Chen Q, Li Q, Liang Y, Zu M, Chen N, Canup BSB, et al. Natural exosome-like nanovesicles from edible tea flowers suppress metastatic breast cancer via ros generation and microbiota modulation. *Acta Pharm Sin B*. 2022;12(2):907-23. <https://doi.org/10.1016/j.apsb.2021.08.016>.
18. Raimondo S, Naselli F, Fontana S, Monteleone F, Lo Dico A, Saieva L, et al. Citrus limon-derived nanovesicles inhibit cancer cell proliferation and suppress cml xenograft growth by inducing trail-mediated cell death. *Oncotarget*. 2015;6(23):19514-27. <https://doi.org/10.18632/oncotarget.4004>.
19. Yang M, Liu X, Luo Q, Xu L, Chen F. An efficient method to isolate lemon derived extracellular vesicles for gastric cancer therapy. *J Nanobiotechnology*. 2020;18(1):100. <https://doi.org/10.1186/s12951-020-00656-9>.

20. Cragg GM, Pezzuto JM. Natural products as a vital source for the discovery of cancer chemotherapeutic and chemopreventive agents. *Med Princ Pract*. 2016;25 Suppl 2(Suppl 2):41-59. <https://doi.org/10.1159/000443404>.
21. Ansary J, Forbes-Hernández TY, Gil E, Cianciosi D, Zhang J, Elexpuru-Zabaleta M, et al. Potential health benefit of garlic based on human intervention studies: A brief overview. *Antioxidants (Basel)*. 2020;9(7). <https://doi.org/10.3390/antiox9070619>.
22. Asemani Y, Zamani N, Bayat M, Amirghofran Z. Allium vegetables for possible future of cancer treatment. *Phytother Res*. 2019;33(12):3019-39. <https://doi.org/10.1002/ptr.6490>.
23. Hsing AW, Chokkalingam AP, Gao YT, Madigan MP, Deng J, Gridley G, et al. Allium vegetables and risk of prostate cancer: A population-based study. *J Natl Cancer Inst*. 2002;94(21):1648-51. <https://doi.org/10.1093/jnci/94.21.1648>.
24. Kumar M, Barbhai MD, Hasan M, Punia S, Dhumal S, Radha, et al. Onion (*allium cepa* L.) peels: A review on bioactive compounds and biomedical activities. *Biomed Pharmacother*. 2022;146:112498. <https://doi.org/10.1016/j.biopha.2021.112498>.
25. Nemzer B, Kalita D. Bioaccessibility, bioavailability, antioxidant activities and health beneficial properties of some selected spices. *IntechOpen*. 2023. <https://doi.org/10.5772/intechopen.109774>
26. Yang Q-Q, Cheng L-Z, Zhang T, Yaron S, Jiang H-X, Sui Z-Q, et al. Phenolic profiles, antioxidant, and antiproliferative activities of turmeric (*curcuma longa*). *Industrial Crops and Products*. 2020;152:112561. <https://doi.org/https://doi.org/10.1016/j.indcrop.2020.112561>.
27. Işahin F, Koçak P, Güneş MY, Özkan İ, Yıldırım E, Kala EY. In vitro wound healing activity of wheat-derived nanovesicles. *Appl Biochem Biotechnol*. 2019;188(2):381-94. <https://doi.org/10.1007/s12010-018-2913-1>.
28. Baddela VS, Nayan V, Rani P, Onteru SK, Singh D. Physicochemical biomolecular insights into buffalo milk-derived nanovesicles. *Appl Biochem Biotechnol*. 2016;178(3):544-57. <https://doi.org/10.1007/s12010-015-1893-7>.
29. Li S, Tu H. Psoralen inhibits the proliferation and promotes apoptosis through endoplasmic reticulum stress in human osteosarcoma cells. *Folia Histochem Cytobiol*. 2022;60(1):101-9. <https://doi.org/10.5603/FHC.a2022.0010>.
30. Franken NA, Rodermond HM, Stap J, Haveman J, van Bree C. Clonogenic assay of cells in vitro. *Nat Protoc*. 2006;1(5):2315-9. <https://doi.org/10.1038/nprot.2006.339>.
31. Han SH, Lee JH, Woo JS, Jung GH, Jung SH, Han EJ, et al. Myricetin induces apoptosis through the mapk pathway and regulates jnk-mediated autophagy in sk-br-3 cells. *Int J Mol Med*. 2022;49(4). <https://doi.org/10.3892/ijmm.2022.5110>.
32. You JY, Kang SJ, Rhee WJ. Isolation of cabbage exosome-like nanovesicles and investigation of their biological activities in human cells. *Bioact Mater*. 2021;6(12):4321-32. <https://doi.org/10.1016/j.bioactmat.2021.04.023>.
33. Bhattacharyya S, Sen P, Wallet M, Long B, Baldwin AS JR, Tisch R. Immunoregulation of dendritic cells by il-10 is mediated through suppression of the pi3k/akt pathway and of ikappab kinase activity. *Blood*. 2004;104(4):1100-9. <https://doi.org/10.1182/blood-2003-12-4302>.
34. Ashaq A, Maqbool MF, Maryam A, Khan M, Shakir HA, Irfan M, et al. Hispidulin: A novel natural compound with therapeutic potential against human cancers. *Phytother Res*. 2021;35(2):771-89. <https://doi.org/10.1002/ptr.6862>.
35. Lu J, Li N, Li S, Liu W, Li M, Zhang M, et al. Biochemical composition, antioxidant activity and antiproliferative effects of different processed garlic products. *Molecules*. 2023;28(2). <https://doi.org/10.3390/molecules28020804>.
36. Roy MK, Kobori M, Takenaka M, Nakahara K, Shinmoto H, Isobe S, et al. Antiproliferative effect on human cancer cell lines after treatment with nimbolide extracted from an edible part of the neem tree (*azadirachta indica*). *Phytother Res*. 2007;21(3):245-50. <https://doi.org/10.1002/ptr.2058>.
37. An Q, van Bel AJ, Hüchelhoven R. Do plant cells secrete exosomes derived from multivesicular bodies? *Plant Signal Behav*. 2007;2(1):4-7. <https://doi.org/10.4161/psb.2.1.3596>.
38. Ju S, Mu J, Dokland T, Zhuang X, Wang Q, Jiang H, et al. Grape exosome-like nanoparticles induce intestinal stem cells and protect mice from dss-induced colitis. *Mol Ther*. 2013;21(7):1345-57. <https://doi.org/10.1038/mt.2013.64>.
39. Xu Z, Xu Y, Zhang K, Liu Y, Liang Q, Thakur A, et al. Plant-derived extracellular vesicles (pdevs) in nanomedicine for human disease and therapeutic modalities. *J Nanobiotechnology*. 2023;21(1):114. <https://doi.org/10.1186/s12951-023-01858-7>.
40. Mu J, Zhuang X, Wang Q, Jiang H, Deng ZB, Wang B, et al. Interspecies communication between plant and mouse gut host cells through edible plant derived exosome-like nanoparticles. *Mol Nutr Food Res*. 2014;58(7):1561-73. <https://doi.org/10.1002/mnfr.201300729>.
41. Wongkaewkhiaw S, Wongrakpanich A, Krobthong S, Saengsawang W, Chairoungdua A, Boonmuen N. Induction of apoptosis in human colorectal cancer cells by nanovesicles from fingerroot (*boesenbergia rotunda* (L.) mansf.). *PLoS One*. 2022;17(4):e0266044. <https://doi.org/10.1371/journal.pone.0266044>.
42. Atale N, Gupta S, Yadav UC, Rani V. Cell-death assessment by fluorescent and nonfluorescent cytosolic and nuclear staining techniques. *J Microsc*. 2014;255(1):7-19. <https://doi.org/10.1111/jmi.12133>.
43. Kaloni D, Diepstraten ST, Strasser A, Kelly GL. Bcl-2 protein family: Attractive targets for cancer therapy. *Apoptosis*. 2023;28(1-2):20-38. <https://doi.org/10.1007/s10495-022-01780-7>.
44. Özkan İ, Koçak P, Yıldırım M, Ünsal N, Yılmaz H, Telci D, et al. Garlic (*allium sativum*)-derived sevs inhibit cancer cell proliferation and induce caspase mediated apoptosis. *Sci Rep*. 2021;11(1):14773. <https://doi.org/10.1038/s41598-021-93876-4>.
45. Carneiro BA, El-Deiry WS. Targeting apoptosis in cancer therapy. *Nat Rev Clin Oncol*. 2020;17(7):395-417. <https://doi.org/10.1038/s41571-020-0341-y>.
46. Thouri A, La Barbera L, Canuti L, Vegliante R, Jelled A, Flamini G, et al. Antiproliferative and apoptosis-inducing effect of common tunisian date seed (var. Korkobbi and arechti) phytochemical-rich methanolic extract. *Environ Sci Pollut Res Int*. 2019;26(36):36264-73. <https://doi.org/10.1007/s11356-019-06606-9>.
47. Liskova A, Koklesova L, Samec M, Smejkal K, Samuel SM, Varghese E, et al. Flavonoids in cancer metastasis. *Cancers (Basel)*. 2020;12(6). <https://doi.org/10.3390/cancers12061498>.
48. Das V, Bhattacharya S, Chikkaputtaiah C, Hazra S, Pal M. The basics of epithelial-mesenchymal transition (emt): A study from a structure, dynamics, and functional perspective. *J Cell Physiol*. 2019;234(9):14535-55. <https://doi.org/10.1002/jcp.28160>.



This work is licensed under a Creative Commons Attribution-Non Commercial 4.0 International License.